21st Australasian Fluid Mechanics Conference
Adelaide, Australia
10-13 December 2018

Direct Numerical Simulation and Large Eddy Simulation of Wind Shear Effects on non-Stratified Open Channel Flow

H. Lashkarbolouk[1], M. P. Kirkpatrick[1], N. Williamson[1], S. W. Armfield[1] and W. Lin[2]

[1]School of Aerospace, Mechanical and Mechatronic Engineering
The University of Sydney, New South Wales 2006, Australia
[2]College of Science & Engineering
James Cook University, Townsville, QLD 4811, Australia

Abstract

In this study, direct numerical simulation (DNS) and large eddy simulation (LES) of turbulent channel flow beneath a flat surface with imposed wind shear stress are presented. An open channel with friction Reynolds number Re_τ= 360 has been considered, while wind shear stresses were imposed as being aligned with the flow direction or not aligned with components in streamwise and spanwise directions. The results indicate that there are differences between wind-driven flow and the case with no wind shear stress. Streaks are present close to the surface in wind-driven flow and profiles of the mean velocity, TKE and mean shear production rate in wind-driven flow are different from those in the unsheared surface flow. Large eddy simulation of wind-driven flow was also carried out to evaluate the performance of sub-grid scale models. It is shown that the features of the flow observed in DNS are well simulated by LES with a relatively small difference near the surface due to shear stress boundary condition.

Introduction

A water body such as a riverine environment or the coastal ocean is affected by a series of forcing mechanisms including tidal flow or wind shear at the air-water interface which lead to momentum transfer and vertical turbulent mixing in the water body. Vertical mixing is important due to its effect on nutrient transport, surface gas exchange, contaminant dispersion and other results of the vertical transport of mass, momentum and heat [1].

Interfacial flows are fluid systems involving immiscible, sheared streams separated by a well-defined continuous interface, such as tidal flow, seawater waves and riverine environments with imposed wind shear [2]. Small scale turbulence near the upper surface is affected by many factors of which the wind shear stress is one of the most important. Accordingly, it is essential for any computational fluid dynamic investigation to consider the effects of wind shear in detail especially when it comes to a study of turbulence close to the fluid-atmospheric interface [3]. Air moving over the surface of a water body involves different turbulence dynamics on the air and water side. Here emphasis is placed on predicting turbulence and fluid dynamics from surface down to the bottom boundary for the water side.

The interaction between turbulence structure and surface related scales of turbulence in interfacial multifluid flows requires the application of high accurate simulation tools such as direct numerical simulation (DNS) and large-eddy simulation (LES).

The sheared interfacial flow considered in this study differs from the unsheared free surface turbulence flow which was studied heretofore in papers such as those of Liu et al. [4], Lombardi et al. [5] and Fulgosi et al. [6]. We model the scenario in which turbulent mixing starts to form under the action of an imposed shear in two directions at the air-water interface. In this case transport processes in the upper part of the water column are different from stress-free surface flows, because the turbulence structure is now controlled by the generation in the near-interface region, and not from the far-field [3].

Study in the field of turbulent channel flow with a sheared surface has not been confined to numerical simulation. Interfacial momentum transfer in a sheared interfacial flow was experimentally studied with an air-water interface by Lorencez et al. [11], Turney and Banerjee [7] and Rashidi and Banerjee [8]. In these studies, the formation of waves on the surface of the water was controlled by experimental techniques, however, some microscale breaking waves were seen in the wind-sheared cases. The investigation of kinematic and turbulence structure of the liquid phase as well as low-speed/high-speed streaks near the surface shows different flow structures and turbulence behaviour in the liquid side in comparison with unsheared turbulent flow.

With regard to numerical simulation, studies can be split into two surface boundary conditions: a flat and a deformable air-liquid interface. In the flat case, the liquid side shows larger velocity fluctuation close to the interface and ejections originate close to the interface [5]. The mean velocity distribution, turbulence intensities, Reynolds stress and various other statistical measures are significantly altered compared to those in the channel without a sheared interface or near the wall region of channel flows [4, 5]. Lam and Banerjee [9] found that the shear rate is much more important than the nature of the boundary conditions in determining the dominant flow structures. They also found that streaks form when the nondimensionalized shear parameter, defined $\tilde{S} \equiv S|\langle u_1' u_3' \rangle|/\epsilon$ where S is the mean shear rate, $\langle u_1' u_3' \rangle$ and ϵ respectively are the kinematic turbulent shear stress and rate of dissipation of turbulent kinetic energy, exceeds unity [9].

Although various efforts have been made to study momentum and mass transfer at the air-liquid interface in more detail, our understanding of turbulence structures near a sheared and wavy interface is not yet fully satisfactory especially when it comes to studying turbulence structure in a more complex case such as turbulent channel flow imposed by wind shear stress not aligned with the flow direction and with components in the streamwise and spanwise directions.

In the present study, we aim to contribute to the discussion regarding sheared interface turbulent flow in an open channel via DNS and LES, solving full time-dependent 3-D Navier-Stokes equations. More especially, this study aims to calculate the mean statistical properties of turbulence near the sheared interface and clarify turbulence mechanisms related to wind shear stress.

Mathematical formulation and numerical method

The physical problem simulated numerically here is the motion of incompressible, Newtonian fluid in a turbulent open channel with shear stress at the surface. An interfacial shear boundary

condition assumes the role of transferring momentum from the air-water interface into the open channel. The spatially filtered Boussinesq equations for conservation of mass and momentum are:

$$\frac{\partial \bar{u}_j}{\partial x_j} = 0, \tag{1}$$

$$\frac{\partial \bar{u}_i}{\partial t} + \bar{u}_j \frac{\partial \bar{u}_i}{\partial x_j} = -\frac{\partial \bar{p}}{\partial x_i} + \frac{1}{Re_\tau}\frac{\partial^2 \bar{u}_i}{\partial x_j^2} - \frac{\partial \tau_{ij}}{\partial x_j}, \tag{2}$$

where x_i, u_i, t and p are the dimensionless coordinate, velocity component, time and pressure respectively which are made dimensionless by their respective scales as follows,

$$u_i = \frac{U_i}{u_\tau};\ x_i = \frac{X_i}{\delta};\ p = \frac{P}{\rho_0 u_\tau^2};\ t = \frac{T.u_\tau}{\delta}, \tag{3}$$

in which the X_i is the dimensional coordinate, U_i the dimensional velocity component, u_τ the wall shear velocity, δ the channel height, and T, P and ρ_0 are the time, pressure, and reference density of the fluid, respectively. The friction Reynolds number is $Re_\tau = u_\tau\delta/\nu$ where ν is kinematic viscosity. The last term in Eq. (2) is the subgrid-scale or SGS stress tensor,

$$\tau_{ij} = \overline{u_i u_j} - \bar{u}_i \bar{u}_j, \tag{4}$$

which represents the unresolved turbulent momentum flux.

A constant uniform shear stress is applied at the upper boundary, while a stationary no-slip boundary condition is used at the bottom of the domain (figure 1). Periodic boundaries are also applied at the side of the domain. The flow in the channel is driven by the combination of the wind shear stress and constant pressure gradient as

$$\Pi = \frac{\tau_{x_i}^s - \tau_{x_i}^w}{\delta}, \tag{5}$$

where $\tau_{x_i}^s$ is the wind shear stress component normalized by the wall shear stress, $\tau_{x_i}^w$.

Results

Cases are defined in table 1 in which Re_τ is the friction Reynolds number, $\tau^s_{x_1}$ and $\tau^s_{x_2}$ are the streamwise and spanwise components of shear stress respectively normalized by the wall shear stress. Case 1 is the direct numerical simulation of turbulent channel flow with shear stress aligned with the flow direction which has been performed in order to check the accuracy of LES. Other cases listed in table 1 have been implemented to study LES of turbulent channel flow with shear stress at the surface either being aligned with the flow direction or not aligned with components in streamwise and spanwise directions. The DNS grid spacing in the streamwise and spanwise directions are respectively $\Delta x_1^+ \approx 10$ and $\Delta x_2^+ \approx 5$, while the stretched grid distribution in the normal direction allows a non-uniform grid size changing from $\Delta x_3^+ \approx 0.25$ at the wall and near the surface to $\Delta x_3^+ \approx 2.5$ in the centre on the channel where $x_3^+ = x_3 u_\tau/\nu$. The grid spacing considered in LES is also two-times coarser than DNS.

Mean velocity profile

Figure 2 shows the profile of the computed mean velocity for $Re_\tau = 360$ normalized by the wall shear velocity. Velocity components are averaged over horizontal planes and time.

In order to verify the velocity profile, the DNS result of the mean velocity distribution in the normal direction for Run 1 is presented in figure 2. It can be found that the LES mean velocity in the streamwise direction closely follows the DNS result throughout the channel. Consequently, the LES formulation employed in the study can be relied upon to accurately predict the mean velocity components in the remaining simulations listed in table 1. With a shear stress at the surface, the mean velocity profile exhibits a different trend in comparison with the flow in a channel without shear stress (Run 2). In contrast with the unsheared case, imposing a shear stress at the upper surface leads to an inflected velocity profile with $d^2\langle u_1\rangle/dx_3^2 > 0$ for $x_3 \geq 0.5$ and rapidly increasing velocity as the surface is approached (the identical behaviour is reported by Walker et al. [1]). More interestingly, the mean velocity in the lower half of the channel with shear stress is smaller than the unsheared surface channel flow. In the lower half of the channel, the mean velocity profiles are quite similar in magnitude in the cases with shear stress component only in the flow direction (Run 3 and Run 5) and shear stress components in the streamwise and spanwise directions (Run 4 and Run 6). Run 5 represents the channel with shear stress as being aligned with the flow direction ($\tau^s_{x_1} = 0.5$). When it comes to the case with shear stress not being aligned with the flow direction and with components in the streamwise and spanwise directions (Run 6), the mean velocity close to the surface is decreased due in part to attenuating effect of spanwise shear component in the momentum equation. In fact when shear stress aligned with the flow direction is imposed (Run 3 & 5), there are zero mean velocity in spanwise direction ($\bar{u}_2 \approx 0$) with low velocity fluctuation ($\bar{u}_2'$). Therefore, the related convective term in Eq. (2) is small with small subgrid scale stress in x_1-x_2 and x_2-x_3 planes. When the shear stress component in the spanwise direction is applied at the surface, the spanwise mean velocity becomes non-zero and the spanwise velocity fluctuation is also increased. This new condition in the channel influences on the related velocity component in the convective and subgrid scale shear stress terms in the momentum equation. Therefore, the streamwise velocity distribution is influenced by the shear stress component in the spanwise direction (Run 4 & 6 in figure 2).

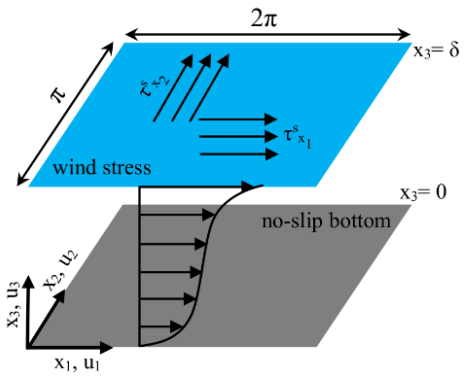

Figure 1. Sketch of three-dimensional DNS and LES domain featuring wind-driven flow over a no-slip bottom.

To study how shear stress affects velocity in the viscous sublayer and logarithmic layer, a semi-logarithmic graph of mean streamwise velocity is shown in figure 3. The curves for the linear region ($\langle u_1\rangle = x^+_3$, for $x^+_3 < 5$) and Nikuradze logarithmic law ($\langle u_1\rangle = (1/\kappa)\ln(x^+_3) + 5.5$, for $x^+_3 > 30$) are also shown where κ is von Kármán constant. The von Kármán constant is 0.41 in this study which concludes a good agreement with $\kappa = 0.40$ reported by Tsai et al. [10]. The velocity profile in the open channel without shear stress at the surface (Run 2) follows these curves with good approximation. The log law region in a turbulent open channel with shear stress at the surface is smaller than this region in the channel without any shear stress as shown in table 2. The log law region in Run 2 extends from $x^+_3 = 30$ to near the surface (h^0 is the length of the

log law region in wall unit which is 330 in Run 2). Table 2 shows the size of log law region in a particular simulation in which C is the Nikuradze logarithmic law constant and h^τ is the length of the log region in the sheared surface flow. It is interesting to note that the upper threshold of the log law region decreases when shear stress not aligned with the flow direction is imposed at the surface of the channel, while the lower threshold of the region is not influenced by shear stress being left at around x^+_3= 30. In another word, the shear stress components forcing the surface of the channel in streamwise and spanwise directions is just able to act on the upper part of the channel (the maximum effect is in Run 4), meanwhile the lower part of the channel and close to the wall reveals the same flow condition regardless of flow condition at the upper part of the channel.

Run	Numerical model	Number of nodes			Re_τ	$\tau^s_{x_1}$	$\tau^s_{x_2}$
		x_1	x_2	x_3			
1	DNS	228	228	181	360	1.0	0.0
2	LES	116	116	89	360	0.0	0.0
3	LES	116	116	89	360	1.0	0.0
4	LES	116	116	89	360	1.0	1.0
5	LES	116	116	89	360	0.5	0.0
6	LES	116	116	89	360	0.5	1.0

Table 1: Matrix of runs performed.

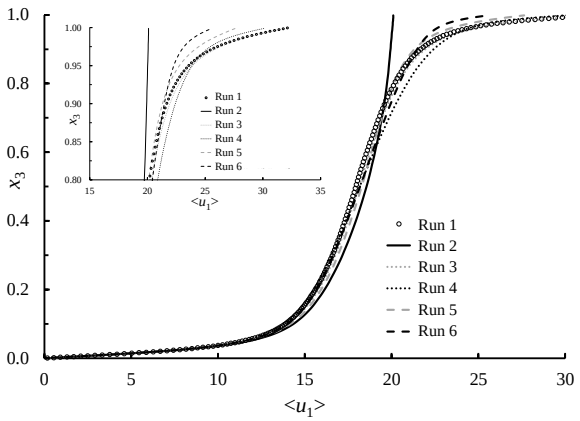

Figure 2. Mean streamwise velocity profiles throughout the channel.

Turbulent kinetic energy and shear production rate

As velocity gradient and turbulent shear stress actively participate in the production of turbulent kinetic energy (TKE) in a channel flow, the mean shear production rate of resolved TKE is investigated in this study defined as below,

$$P = -\langle \bar{u}_i' \bar{u}_j' \rangle \frac{\partial \langle \bar{u}_i \rangle}{\partial x_j}, \qquad (6)$$

where $\bar{u}_i'$ is the velocity fluctuation component in i direction (Walker et al., [1]). In a turbulent open channel flow, the mean kinetic energy per unit mass is also defined as turbulent kinetic energy associated with eddies in the channel. Physically, the root mean square of velocity fluctuation characterizes TKE as below,

$$\bar{q} = \frac{1}{2} \langle \bar{u}_i' \bar{u}_i' \rangle. \qquad (7)$$

In fact, when velocity gradient changes in the velocity profile, the related velocity fluctuation changes as well leading to generation of TKE.

In this regard, figures 4 & 5 respectively show the distribution of the mean shear production rate and TKE throughout the channel for cases listed in table 1. Close to the surface of the unsheared surface flow, the mean velocity gradient is small (Run 2 in figure 2) promoting the small value of streamwise velocity fluctuation. Therefore, the mean shear production rate is inclined to lessen approaching the surface and becomes zero at the surface due to the zero normal velocity component. By imposing shear stress at the surface of the channel aligned with the flow direction (Run 3 & 5), the velocity gradient in the upper half of the channel is increased leading to growth in the streamwise velocity fluctuation. In figure 4, it can be clearly seen that the mean shear production in the channel flow is significantly higher in Run 3 with $\tau^s_{x_1}$= 1.0 and Run 5 with $\tau^s_{x_1}$= 0.5 in comparison with Run 2 especially near the surface. As the streamwise velocity fluctuation increases in the sheared interface case, we can expect a rise in the TKE which is apparent in figure 5.

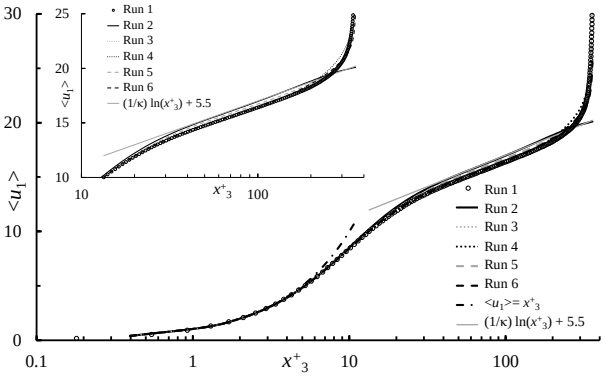

Figure 3. Log law profiles of the mean streamwise velocity.

Run	κ	C	Log layer area (h^τ)	R_{log}= h^τ/h^0
1	0.41	4.9	$30 < h^\tau < 200$	0.52
3		5.1	$30 < h^\tau < 190$	0.48
4		4.8	$30 < h^\tau < 130$	0.30
5		5.2	$30 < h^\tau < 200$	0.52
6		5.0	$30 < h^\tau < 150$	0.36

Table 2. The von Kármán and Nikuradze logarithmic law constants in the designed simulations. h^τ and R_{log} show the log layer extent and the ratio of log layer extent for sheared surface flow over unsheared surface case, respectively.

The surface shear stress component in the spanwise direction makes a slight change in the mean streamwise velocity, as discussed in the previous section and figure 2. While this event slightly reduces the streamwise velocity fluctuation, it leads to a mean spanwise velocity component and an increase in the spanwise velocity fluctuation. Consequently and with regard to the increase in the spanwise velocity fluctuation, the shear production rate in Run 4 & 6 with shear stress components in the streamwise and spanwise directions ($P = -\langle \bar{u}_1' \bar{u}_3' \rangle \partial \langle \bar{u}_1 \rangle / \partial x_3 - \langle \bar{u}_2' \bar{u}_3' \rangle \partial \langle \bar{u}_2 \rangle / \partial x_3$) is higher than the cases without the spanwise shear stress component from $x_3 >$ 0.2 up to the surface, with the peak just beneath the surface in figure 4. The shear production becomes zero at the surface because of the impermeable boundary condition.

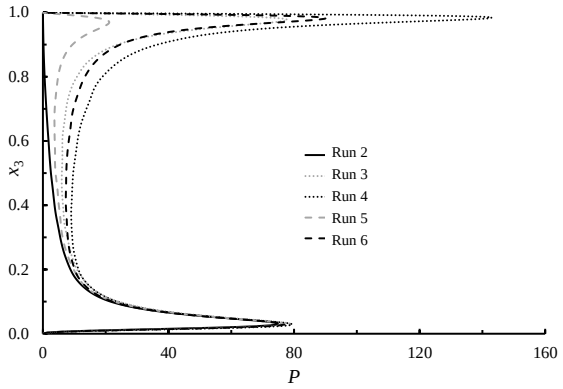

Figure 4. Shear production term in turbulent kinetic energy equation.

Figure 5 shows that TKE is increased in the simulations with the shear stress components in the streamwise and spanwise directions. As the spanwise velocity fluctuation is increased by imposing the shear stress component in that direction, the related term in the turbulent kinetic energy (Eq. (7)) is increased leading to higher values of TKE in the channel than the cases without shear stress component in the spanwise direction. It is shown that TKE in the whole channel is increased by having shear stress components in two directions at the surface and helps the channel to be well mixed.

In figure 5 a comparison among TKE of the DNS (Run 1) and LES (Run 3) is presented in order to check the validity of the large eddy simulation in computing TKE and velocity fluctuation components in a fully turbulent flow with sheared surface. While the LES results are in good agreement with the DNS just above the wall, there are some relatively small differences between the LES and DNS especially near the surface. These differences are due to the boundary conditions applied at the wall and surface. While a no-slip boundary condition is applied at the wall, a constant uniform shear stress is applied at the surface. It appears that LES does not capture turbulence close to the sheared boundary condition as well as it captures wall turbulence.

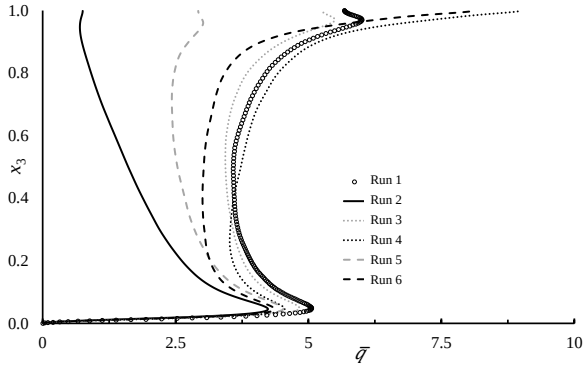

Figure 5. Turbulent kinetic energy distribution in no-sheared and sheared turbulent interfacial flow.

Conclusions

Turbulent open channel flow with an imposed shear stress at the surface representing wind shear was investigated. The effects of changing in the wind direction have been examined by imposing shear stress components in different directions at the surface. Wind stress at the interface changes physical processes in many ways by altering mean and fluctuation terms of parameters such as velocity in the open channel. It is observed that the extent of log law region is decreased in the sheared surface flow compared with the unsheared one ($R_{log} \approx 0.5$ for the cases with the shear stress as being aligned with the flow direction and $R_{log} \approx 0.3$ in the cases with shear stress not aligned with the flow direction and with components in streamwise and spanwise directions). More interestingly, the wind shear stress components in two directions affects a higher portion of the turbulent open channel by changing the mean and fluctuation distribution of velocity which influences the momentum transfer and vertical turbulent mixing in the channel. The highest TKE and mean shear production rate are seen in Run 4 with $\tau^s_{x_1} = 1.0$ and $\tau^s_{x_2} = 1.0$ while the lowest values of these parameters are found in unsheared surface flow.

References

[1] Walker, R., Tejada-Martínez, A.E., & Grosch, C.E., Large-eddy simulation of a coastal ocean under the combined effects of surface heat fluxes and full-depth Langmuir circulation, *Journal of Physical Oceanography*, **46(8)**, 2016, 2411-2436.

[2] Reboux, S., Sagaut, P., & Lakehal, D., Large-eddy simulation of sheared interfacial flow, *Physics of Fluids*, **18(10)**, 2006, 105105.

[3] Enstad, L.I., Nagaosa, R., & Alendal, G., Low shear turbulence structures beneath stress-driven interface with neutral and stable stratification, *Physics of Fluids*, **18(5)**, 2006, 055106.

[4] Liu, S., Kermani, A., Shen, L., & Yue, D.K., Investigation of coupled air-water turbulent boundary layers using direct numerical simulations, *Physics of Fluids*, **21(6)**, 2006, 062108.

[5] Lombardi, P., De Angelis, V., & Banerjee, S., Direct numerical simulation of near-interface turbulence in coupled gas-liquid flow, *Physics of Fluids*, **8(6)**, 1996, 1643-1665.

[6] Fulgosi, M., Lakehal, D., Banerjee, S., & De Angelis, V., Direct numerical simulation of turbulence in a sheared air–water flow with a deformable interface, *Journal of fluid mechanics*, **482**, 2003, 319-345.

[7] Turney, D.E., & Banerjee, S., Air–water gas transfer and near-surface motions, *Journal of Fluid Mechanics*, **733**, 2013, 588-624.

[8] Rashidi, M.T., & Banerjee, S., The effect of boundary conditions and shear rate on streak formation and breakdown in turbulent channel flows, *Physics of Fluids A: Fluid Dynamics*, **2(10)**, 1990, 1827-1838.

[9] Lam, K., & Banerjee, S., On the condition of streak formation in a bounded turbulent flow. *Physics of Fluids A: Fluid Dynamics*, **4(2)**, 1992, 306-320.

[10] Tsai, W.T., Chen, S.M., Lin, M.Y., & Hung, L.P., Molecular sublayers beneath the air-sea interface relative to momentum, heat and gas transports, *Geophysical research letters*, **30(18)**, 2003, 1968.

[11] Lorencez, C., Nasr-Esfahany, M., Kawaji, M., & Ojha, M., Liquid turbulence structure at a sheared and wavy gas-liquid interface, *International journal of multiphase flow*, **23(2)**, 1997, 205-226.